UCRL-18234

Cy. 2

University of California
Ernest O. Lawrence Radiation Laboratory

TWO-WEEK LOAN COPY

This is a Library Circulating Copy which may be borrowed for two weeks. For a personal retention copy, call Tech. Info. Division, Ext. 5545

ANALYSIS OF GAS-SOLID SURFACE KINETIC MODELS USING LOCK-IN DETECTION OF MODULATED MOLECULAR BEAMS

D. R. Olander

(June 1968)

RECEIVED
LAWRENCE
RADIATION LABORATORY
JUL 23 1968
LIBRARY AND
DOCUMENTS SECTION

Berkeley, California

UCRL 18234

DISCLAIMER

This document was prepared as an account of work sponsored by the United States Government. While this document is believed to contain correct information, neither the United States Government nor any agency thereof, nor the Regents of the University of California, nor any of their employees, makes any warranty, express or implied, or assumes any legal responsibility for the accuracy, completeness, or usefulness of any information, apparatus, product, or process disclosed, or represents that its use would not infringe privately owned rights. Reference herein to any specific commercial product, process, or service by its trade name, trademark, manufacturer, or otherwise, does not necessarily constitute or imply its endorsement, recommendation, or favoring by the United States Government or any agency thereof, or the Regents of the University of California. The views and opinions of authors expressed herein do not necessarily state or reflect those of the United States Government or any agency thereof or the Regents of the University of California.

UCRL-18234
Preprint

Paper presented at:
Fourth International Materials Symposium
June 19-22, 1968

UNIVERSITY OF CALIFORNIA
Lawrence Radiation Laboratory
Berkeley, California

AEC Contract No. W-7405-eng-48

ANALYSIS OF GAS-SOLID SURFACE KINETIC MODELS USING LOCK-IN DETECTION OF MODULATED MOLECULAR BEAMS

D. R. Olander

(June 1968)

ANALYSIS OF GAS-SOLID SURFACE KINETIC MODELS USING LOCK-IN DETECTION OF MODULATED MOLECULAR BEAMS

D. R. Olander

Inorganic Materials Research Division, Lawrence Radiation Laboratory,
Department of Nuclear Engineering, University of California,
Berkeley, California

ABSTRACT

The analytical techniques for extracting surface rate constants from the amplitude and phase shift data provided by the lock-in amplifier are developed for several types of gas-solid interactions. Based upon a particular model, the response of the surface emission rate of a particular reaction product or intermediate to the square wave input of the reactant gas molecular beam is calculated. The fundamental mode of the Fourier transform of the emission rate waveform is then determined. This mathematical step represents the operation of the lock-in detector on the output of the mass spectrometer. The analytical methods are applied to the following processes:

1) Slow, competitive first and second order surface reactions. The effect of the background gas on the response of the lock-in detector is described.

2) Two slow, competitive first order reactions each of which is followed by a slow desorption step. While data from a modulated beam experiment can in principle determine all four of the rate constants involved, the equivalent dc molecular beam experiment provides only the ratio of two of the rate constants.

3) Competition between rapid first order desorption and solution and diffusion of the adsorbed atoms in the bulk solid. The balances

appear as boundary conditions for the diffusion equation in the bulk medium.

4) competition between first order desorption and surface migration.

INTRODUCTION

Heterogeneous chemical kinetic studies by modulated molecular beam mass spectrometry have been made possible by the development within the past decade of three important experimental tools: high sensitivity, compact mass spectrometers; ultra-high vacuum techniques and clean, high speed vacuum pumps; and sources for the generation of intense molecular beams. The reactant gas interacts with the solid surface as a collimated beam of particles rather than as a randomly directed flux. The products of the interaction are monitored by a mass spectrometer located in the vacuum system. The molecular beam is chopped or modulated to permit detection by phase-sensitive amplification, which greatly improves the signal-to-noise ratio.

A major advantage of the molecular beam-mass spectrometric method of investigating heterogeneous chemical kinetics is that very reactive free radical intermediates of the reaction can be analyzed as readily as stable products. Knowledge of the nature and concentration of these intermediates is of considerable assistance in elucidating reaction mechanisms. Sampling by molecular beams in a high vacuum insures that the observed species represent primary products of the surface reaction, and not stable species resulting from wall or gas phase collisions prior to analysis.

Experiments of this type determine the identity of the primary products of the reaction, the fraction of the incident reactant molecules which ultimately return to the gas as a particular reaction product, and the average residence time of the product species on the solid surface. The controllable experimental parameters are: the

intensity of the molecular beam (or the equivalent pressure of the gaseous reactant); the temperature of the molecular beam; the temperature of the solid surface; the composition of the beam, and the modulation frequency. The dissociation of hydrogen on tungsten and the reaction of chlorine with nickel have been studied in this manner.[1]

The apparatus shown in Fig. 1 has been used to investigate the hydrogen-tantalum system[2] and is typical of systems which have been employed or are being constructed for studies of this type. The system consists of two vacuum chambers. The chamber on the left of Fig. 1 contains the molecular beam source, the efflux from which is mechanically modulated by a small rotating toothed disk. The small fraction of the gas effusing from the source which passes through the small orifice connecting the two chambers constitutes the modulated molecular beam. The solid target and the mass spectrometer are shown in the larger vacuum chamber on the right of Fig. 1.

The heart of the detection system is the phase sensitive or lock-in amplifier. The output signal from the mass spectrometer first goes through a preamplifier, then an intermediate amplifier where the entire spectrum of frequencies is amplified, and then through a signal-tuned amplifier which limits the signal to a narrow bandwidth centered on the frequency of the chopped primary molecular beam. The signal is then mixed with the first harmonic of the reference signal in a synchronous demodulator to produce a rectified ac signal which passes through an integrating circuit to produce a dc output. When employed in this manner, the lock-in amplifier produces two independent pieces of information: the amplitude of the output signal and its phase difference compared to some selected signal.

The absolute magnitude of the amplitude of the signal is generally not of interest. To relate the amplitude directly to the absolute rate of emission from the surface requires knowledge of the fraction of the emission from the surface intercepted by the electron beam of the mass spectrometer, ionization cross sections and extraction and transmission efficiencies of the mass spectrometer, and the gain of the electron multiplier. At best, such estimates are accurate to no more than a factor of 2-3.[3] However, the percentage change in the output signal amplitude at a particular mass number as experimental conditions are varied can provide quantitative kinetic information. This relative amplitude contains two factors; the "competition factor" represents an actual change in the average rate of emission of a particular species from the surface due to effects such as competitive reactions or diffusional processes. The second factor is determined by the response of the lock-in amplifier to the shape and amplitude of the ac portion of the modulated signal waveform. This "demodulation factor" is directly related to the ratio of the average residence time on the surface to the chopping time, and hence to the phase lag of the signal. The amplitude of the output signal is most conveniently measured relative to the signal when the surface interaction is sufficiently simple to be considered completely interpretable. In the case of simple dissociation of diatomic gases on metals, for example, the reference situation might be the output signal when the target is at temperatures high enough to instantaneously re-evaporate as atoms all of the molecular gas which chemisorbs.

The phase shift is most conveniently measured with respect to experimental conditions under which the residence time of the molecules on the surface is small compared to the modulation frequency (e.g., residence times on the order of 10^{-4} sec or less). For noncondensible gases, this could be a room temperature beam scattered from a room temperature target. Provided that the transit time between the target and the ion source is small, the shift in phase of the output signal of a product species is indicative of reaction times which are of the same order of magnitude as the modulation time. Generally, phase shift data provide information on the absolute magnitude of the rate constants of the elementary surface processes, whereas relative amplitude data (after correction for the demodulation factor) provide information on the ratio of rate constants due to competing surface reactions. In non-modulated (dc) experiments such as those of McKinley,[4] only the latter type of information is obtainable.

Yamamoto and Stickney[5] have recently analyzed the response of the lock-in detector to molecular beams which undergo simple scattering at the solid target. Although the process of slow first order desorption was considered briefly, the emphasis was on the velocity distribution of the scattered molecules. In this study, we consider surface processes more complex than scattering or simple first order desorption, but assume molecular flight times between the target and the mass spectrometer to be small compared to the modulation time. All species are assumed to be emitted from the surface at the temperature of the surface and in a diffuse manner. Since the ionization efficiency of the mass spectrometer is proportional to the inverse of the mean speed

of the molecules, the product of the square root of the surface temperature, T_T, and the instantaneous output signal from the mass spectrometer, $S_i(t)$, is assumed proportional to the instantaneous rate of emission of a species from the surface $R_i^E(t)$:

$$\sqrt{T_T}\, S_i(t) = \alpha_i R_i^E(t) \qquad (1)$$

The constant of proportionality α_i depends upon the ionization cross section, extraction and transmission efficiencies of the mass analyzer, and electron multiplier sensitivity for species i. Intercomparison of different species requires calibration of the mass spectrometer, as indicated by Smith and Fite.[1]

The output current from the mass spectrometer, $S_i(t)$, is dropped over the R ohm input impedance of the preamplifier of the lock-in detector; this periodic signal is then Fourier analyzed and only the fundamental mode retained. RMS averaging of the synchronous demodulator output by the RC filter used as a final stage of the lock-in amplifier leads to an additional reduction of the signal by $\sqrt{2}$. The dc output of the lock-in detector V_i can be written as

$$V_i = \frac{R}{\sqrt{2}} \mathcal{F}\{S_i(t)\} = \frac{R}{\sqrt{2}} \frac{\alpha_i}{\sqrt{T_T}} \mathcal{F}\{R_i^E(t)\} \qquad (2)$$

where $\mathcal{F}\{S_i(t)\}$ represents the operation of the Fourier analyzing a periodic signal and retaining only the fundamental mode. It is assumed that the phase angle of the reference signal has been adjusted to

maximize the dc output of the lock-in unit; the magnitude of the adjustment required for a particular signal compared to the adjustment required for a signal from a surface interaction process of zero residence time is the phase shift, and is denoted by ϕ_i. The maximized dc output of the lock-in detector, corrected for mass spectrometer effects associated with target temperature and species discrimination is called the amplitude of species i and is denoted by $\mathcal{A}_i$:

$$\mathcal{A}_i = \frac{\sqrt{2}}{R} \frac{\sqrt{T_T V_i}}{\alpha_i} = \mathcal{F}\{R_i^E(t)\} \qquad (3)$$

The periodic nature of the surface emission rate is due to the regular interruption of the primary molecular beam of reactant gas by a mechanical chopper. If the molecular transit time between the molecular beam source and the detector is small compared to the chopping time, the primary modulated beam can be represented by a square wave. Figure 2 shows an oscilloscope trace of a 145 cps primary beam of molecular oxygen measured by a mass spectrometer 4.5 cm from the effusion source. The amplitude of the primary beam striking the solid, I_T^o molecules/cm^2-sec, is proportional to the height of the square wave in Fig. 2. The modulated beam intensity is analagous to the reactant gas pressure in conventional rate experiments.

For molecular beams of non-condensible species such as H_2, O_2, or CO, the background gas in the vacuum chamber containing the target consists primarily of the same species as the beam itself. In addition to the modulated molecular beam, the target is also subject to a steady bombardment of reactant from the background gas. This contribution to

the total reactant gas impingement rate is denoted by I^{bkg} molecules/cm^2-sec., and can be calculated from pressure measurements and simple kinetics theory formulae. The total rate at which each cm^2 of target is struck by reactant molecules is

$$I_T(t) = I_T^o \, [f^o(t) + 1/\rho] \qquad (4)$$

where $f^o(t)$ is a square wave of unit amplitude at the modulation frequency and ρ is the beam-to-background impingement rate ratio I_T^o/I^{bkg}.

For first order surface processes, the background contribution in Eq. (4) does not affect the interpretation of the lock-in detector data, since it represents a dc signal to which the lock-in system does not respond. For non-linear surface processes, however, the background impingement increases the supply of adsorbed atoms on the surface with which the molecular beam can react. In this situation, the background contributes in an intimate manner to the product emission rate.

The flux of a species from the surface is related in a simple way to the concentration of that species or its precursor on the surface. The response of the lock-in system can be computed in terms of the time variation of an adsorbed species on the surface. A sketch of the change of the surface concentration of an adsorbed species during a complete modulation cycle is shown in Fig. 3. Here, t_c denotes the chopping time, which is the reciprocal of twice the modulation frequency. During the "on" portion of the cycle ($-t_c < t < 0$) the surface concentration grows due to the supply of reactants from the beam. During the "off" portion of the cycle ($0 < t < t_c$) the surface population diminishes due to removal of the adsorbed layer by direct evaporation, reaction, or other

loss processes. These mechanisms are of course operative during the "on" part of the cycle as well, but here the supply rate from the beam is greater than the removal rates. During the "on" period, the driving function $f^{o}(t)$ is constant at unity, and during the "off" portion of the cycle, the driving function is zero. The time variation of an adsorbed species can be calculated by solving the appropriate differential equations representing surface mass balances for all of the adsorbed species. The resulting function is then Fourier analyzed and the coefficients of the fundamental mode identified. In order to relate the phase shift ϕ_i and the amplitude $\mathcal{A}_i$ to the periodic behavior of the surface concentration, a specific model of the surface processes must be chosen.

I. Slow, Competitive First and Second Order Surface Reactions

This process represents the atomization of a diatomic gas on (typically) a metal surface. The elementary reactions can be written as

$$X_2(g) \longrightarrow 2X(a)$$
$$X(a) \xrightarrow{k_1^E} X(g)$$
$$2X(a) \xrightarrow{k_2^E} X_2(g)$$

The first reaction represents dissociative chemisorption, which proceeds at a rate equal to the product of the sticking probability η_2 and the impingement rate given by Eq. (4). The second reaction represents direct evaporation of the adsorbed atoms, and the last reaction represents bimolecular surface reconstitution and evaporation of molecules. If the surface concentration of X is denoted by n, a

mass balance on the surface yields:

$$\frac{dn}{dt} = 2\eta_2 I_T^\circ [f^\circ(t) + 1/\rho] - k_1^E n - 2k_2^E n^2 \tag{5}$$

where k_1^E and k_2^E are the rate constants for the atom and molecule evaporation steps, respectively. Dimensionless parameters are defined by:

$$N = \frac{k_1^E n}{\eta_2 I_T^\circ} \tag{6}$$

$$\theta = 2k_1^E t \tag{7}$$

$$b = 16 \frac{\eta_2 I_T^\circ}{(k_1^E)^2/k_2^E} \tag{8}$$

and Eq. (5) written as

$$\frac{dN}{d\theta} = f^\circ(\theta) + 1/\rho - \frac{1}{2}N - \frac{1}{16} bN^2 \tag{9}$$

Equation (9) can be solved by direct integration. During the "on" part of the cycle, $f^\circ(\theta) = 1$, and the solution is:

$$N_{on}(\theta) = \frac{4}{b}\left\{[1+b(1+1/\rho)]^{1/2} \tanh\{\tfrac{1}{4}[1+b(1+1/\rho)]^{1/2}(\theta+C_{on})\} - 1\right\} \tag{10}$$

Similarly, for the "off" portion of the cycle, $f^\circ(\theta) = 0$, and the solution is:

$$N_{off}(\theta) = \frac{4}{b}\left\{[1+b(1/\rho)]^{1/2} \operatorname{ctnh}\{\tfrac{1}{4}[1+b(1/\rho)]^{1/2} (\theta+C_{off})\} - 1\right\} \tag{11}$$

The constants of integration C_{on} and C_{off} are determined by applying matching conditions representing the cyclic steady state nature of the process:

$$N_{on}(0) = N_{off}(0)$$
$$N_{on}(-\theta_c) = N_{off}(\theta_c) \tag{12}$$

which yield

$$[1+b(1+1/\rho)]^{1/2} \tanh\left\{\frac{1}{4}[1+b(1+1/\rho)]^{1/2}\, C_{on}\right\}$$
$$= [1+b(1/\rho)]^{1/2} \operatorname{ctnh}\left\{\frac{1}{4}[1+b(1/\rho)]^{1/2}\, C_{off}\right\} \tag{13}$$

$$[1+b(1+1/\rho)]^{1/2} \tanh\left\{\frac{1}{4}[1+b(1+1/\rho)]^{1/2}\, (-\theta_c+C_{on})\right\}$$
$$= [1+b(1/\rho)]^{1/2} \operatorname{ctnh}\left\{\frac{1}{4}[1+b(1/\rho)]^{1/2}\, (\theta_c+C_{off})\right\} \tag{14}$$

These two equations must be solved numerically for C_{on} and C_{off} as functions of the parameters b, $1/\rho$, and θ_c.

The rate of evaporation of X(a) (species X denoted by subscript 1) is:

$$R_1^E(t) = k_1^E n(t) \tag{15}$$

Combining Eqs. (3), (6), and (15), the amplitude of the output signal is:

$$\mathcal{A}_1 = \eta_2 I_T^\circ \mathcal{F}[N(\theta)] \tag{16}$$

If the coefficients of the fundamental terms of the Fourier expansion of $N(\theta)$ are denoted by A and B, the amplitude and phase shift are:

$$\mathcal{A}_1 = \eta_2 I_T^{\circ}(A^2 + B^2)^{1/2} \tag{17}$$

$$\phi_1 = \tan^{-1}(A/B) \tag{18}$$

where

$$A = \frac{1}{\theta_c}\int_{-\theta_c}^{0} N_{on}(\theta)\cos\left(\frac{\pi\theta}{\theta_c}\right) d\theta + \frac{1}{\theta_c}\int_{0}^{\theta_c} N_{off}(\theta)\cos\left(\frac{\pi\theta}{\theta_c}\right)d\theta \tag{19}$$

$$B = \frac{1}{\theta_c}\int_{-\theta_c}^{0} N_{on}(\theta)\sin\left(\frac{\pi\theta}{\theta_c}\right) d\theta + \frac{1}{\theta_c}\int_{0}^{\theta_c} N_{off}(\theta)\sin\left(\frac{\pi\theta}{\theta_c}\right)d\theta \tag{20}$$

Inserting Eqs. (11) and (12) into (19) and (20) yields:

$$A = \frac{4}{\pi}\frac{1}{b}\left\{\epsilon_{on} J_{A_{on}}\left(\frac{\epsilon_{on}\theta_c}{4\pi}, \frac{\epsilon_{on}C_{on}}{4}\right) + \epsilon_{off} J_{A_{off}}\left(\frac{\epsilon_{off}\theta_c}{4\pi}, \frac{\epsilon_{off}C_{off}}{4}\right)\right\} \tag{21}$$

$$B = \frac{4}{\pi}\frac{1}{b}\left\{\epsilon_{on} J_{B_{on}}\left(\frac{\epsilon_{on}\theta_c}{4\pi}, \frac{\epsilon_{on}C_{on}}{4}\right) + \epsilon_{off} J_{B_{off}}\left(\frac{\epsilon_{off}\theta_c}{4\pi}, \frac{\epsilon_{off}C_{off}}{4}\right)\right\} \tag{22}$$

where

$$\begin{aligned} \epsilon_{on} &= [1 + b(1 + 1/\rho)]^{1/2} \\ \epsilon_{off} &= [1 + b(1/\rho)]^{1/2} \end{aligned} \tag{23}$$

and the J's are the integrals:

$$J_{Aon}(x,y) = \int_{-\pi}^{0} \tanh(xu+y) \cos u \, du \tag{24}$$

$$J_{Aoff}(x,y) = \int_{0}^{\pi} \operatorname{ctnh}(xu+y) \cos u \, du \tag{25}$$

$$J_{Bon}(x,y) = \int_{-\pi}^{0} \tanh(xu+y) \sin u \, du \tag{26}$$

$$J_{Boff}(x,y) = \int_{0}^{\pi} \operatorname{ctnh}(xu+y) \sin u \, du \tag{27}$$

these integrals cannot be evaluated in closed form.

For this reaction sequence, it is convenient to relate the amplitude of the output singal to the value when $k_1^E \gg 1/t_c$, $k_1^E \gg k_2^E$, which generally occurs at high target temperatures. In dimensionless terms, these conditions imply $\theta_c \to \infty$ and $b \to 0$. The coefficients A and B reduce to 0 and $-4/\pi$, respectively, and:

$$\left[\mathcal{Q}_1\right]_{\substack{b=0 \\ \theta_c=\infty}} = \frac{4}{\pi} \eta_2 I_T^{\circ} \tag{28}$$

$$\left[\phi_1\right]_{\substack{b=0 \\ \theta_c=\infty}} = 0 \tag{29}$$

These results could have been obtained directly from Eq. (9) by dropping the first and last terms.

Equations (13), (14), (21), and (22) have been utilized to calculate A and B as functions of b and θ_c for $1/\rho = 0$. The results are plotted in Figs. 4 and 5 as the phase shift of Eq. (18) and the amplitude attenuation, defined as the ratio of Eq. (17) to Eq. (28). These two plots show the effect of competition between the first and second order processes through the parameter b and the speed of the evaporation reaction compared to the modulation time through the parameter θ_c. If both the amplitude attenuation and the phase shift are experimentally accessible, both k_1^E and k_2^E can be determined individually.

I(a) Rapid Competitive First and Second Order Reactions

This system is a special case of the slow competitive first and second order reactions considered above. It is typical of the adsorption of hydrogen on refractory metals.[1,2] The residence time of hydrogen on the surface $(1/k_1^E)$ is small compared to typical modulation times, so that $\theta_c \to \infty$. However, over much of the target temperature range, atom evaporation and molecular reconstitution are of comparable magnitude, so that the parameter b is not zero. Since the phase shift is always zero, all information on the absolute magnitudes of k_1^E and k_2^E is lost. Only amplitude attenuation data remains to provide information on the ratio of these rate constants.

Since $\theta_c \to \infty$, θ also approaches ∞ and the hyperbolic tangent and cotangent terms in Eqs. (10) and (11) reduce to unity. The functions N_{on} and N_{off} become constants over their respective intervals and the coefficients A and B are easily evaluated from Eqs. (19) and (20). There results:

$$A = 0$$

$$B = \frac{8}{\pi b} \left\{ [1 + b(1 + 1/\rho)]^{1/2} - [1 + b(1/\rho)]^{1/2} \right\}$$

The amplitude attenuation is

$$\frac{[\mathcal{A}_1]_{\theta_c=\infty}}{[\mathcal{A}_1]_{\substack{b=0 \\ \theta_c=\infty}}} = \frac{2}{b} \left\{ [1 + b(1 + 1/\rho)]^{1/2} - [1 + b(1/\rho)]^{1/2} \right\} \quad (30)$$

This equation (with $1/\rho = 0$) is well represented by the $\theta_c = 500$ curve of Fig. 4. Provided the model is correct, the data permit the parameter b to be evaluated from Eq. (30), and from b, the rate constant ratio $(k_1^E)^2/k_2^E$. In general, the amplitude attenuation does not vary either as the first power or the square root of the equivalent beam pressure, which is contained in the parameter b. These limits are approached asympotically at large and small values of b. Equation (30) demonstrates the importance of quantitative knowledge of the beam-to-background ratio in interpreting lock-in detector data for processes involving a second order surface step.

I(b) Slow First Order Desorption

This limiting case is applicable to the desorption of cesium from tungsten, which has been studied by Perel, Vernon, and Daley.[6] Since no second order surface processes are present, b = 0, but since the residence time on the surface is comparable to the chopping time, θ_c

is finite. Since N_{on} and N_{off} must remain finite, the hyperbolic tangents and cotangents in Eqs. (10) and (11) must approach unity. They do so because C_{on} and C_{off} become large. Approximating tanh(x) by $1 - 2e^{-2x}$ and $(1 + x)^{1/2}$ by $1 + x/2$, the matching conditions Eqs. (13) and (14) yield:

$$e^{-1/2C_{on}} = \frac{b}{4} \frac{e^{-\theta_c/2}}{1 + e^{-\theta_c/2}}$$

$$e^{-1/2C_{off}} = \frac{b}{4} \frac{1}{1 + e^{-\theta_c/2}}$$

The integrals involved in Eqs. (21) and (22) can be evaluated analytically to yield:

$$A = \frac{4}{\pi} \frac{\pi(\frac{1}{2}\theta_c)}{\pi^2 + (\frac{1}{2}\theta_c)^2} \tag{31}$$

$$B = -\frac{4}{\pi} \frac{(\frac{1}{2}\theta_c)^2}{\pi^2 + (\frac{1}{2}\theta_c)^2} \tag{32}$$

the phase lag is:

$$\phi_1 = \tan^{-1}\left(-\frac{\pi}{\frac{1}{2}\theta_c}\right) \tag{33}$$

and the amplitude attenuation is:

$$\frac{\left[\mathcal{A}_1\right]_{b=0}}{\left[\mathcal{A}_1\right]_{\substack{b=0\\ \theta_c=\infty}}} = \frac{\frac{1}{2}\theta_c}{[\pi^2+(\frac{1}{2}\theta_c)^2]^{1/2}} \tag{34}$$

Equations (33) and (34) are identical to the expressions obtained by Perel et al.[6] Their method, however, is not easily adapted to the general case in which second order processes compete with first order desorption.

II. The Nickel-Chlorine Reaction

This relatively simple gas-solid reaction is the only heterogeneous reaction involving volatilization of the solid substrate which has been studied by modulated molecular beam techniques. Smith and Fite[1] report preliminary data on the amplitude and phase shift of the NiCl product signal. McKinley[4] has performed a dc beam experiment on the same system and reported amplitude data for both NiCl and $NiCl_2$. Both of these studies present signal amplitude data in arbitrary units, so that kinetic information can only be obtained from the amplitude attenuation factors discussed previously.

McKinley has shown that the amplitude of the NiCl and $NiCl_2$ signals are proportional to the beam strength, so that all reactions are first order with respect to chlorine concentration. His data indicate that the sum of the NiCl signal and twice the $NiCl_2$ signal is constant. This suggests that the instrumental constant α in Eq. (1) is the same

for NiCl and $NiCl_2$, and that adsorbed chlorine leaves the surface only as one of the two nickel-bearing species. Based upon these observations, McKinley's model for the surface process is:

$$
\begin{array}{lcl}
 & & \xrightarrow{k_c p_c} 2NiCl(a) \xrightarrow{k_1^E} NiCl(g) \\
2Ni + Cl_2(g) \longrightarrow (NiCl)_2 & & \\
 & & \xrightarrow[k_c(1-p_c)]{} NiCl_2(a) \xrightarrow{k_2^E} NiCl_2(g) \\
 & & \quad + Ni
\end{array}
$$

where $1/k_c$ is the mean lifetime of the complex $(NiCl)_2$ on the surface and p_c is the probability of complex decomposition to adsorbed NiCl. The parameters k_c and p_c are analogous to the half-life and branching ratio used to describe radioactive decay. The rate constants k_1^E and k_2^E are the reciprocals of the mean lifetimes of the adsorbed species NiCl(a) and $NiCl_2(a)$.

If the surface concentrations of $(NiCl)_2$, NiCl(a) and $NiCl_2(a)$ are denoted by n_c, n_1, and n_2 respectively, balances on these three species are:

$$\frac{dn_c}{dt} = \eta_2 I_T^\circ [f^\circ(t) + 1/\rho] - k_c n_c \tag{35}$$

$$\frac{dn_1}{dt} = 2k_c p_c n_c - k_1^E n_1 \tag{36}$$

$$\frac{dn_2}{dt} = k_c(1 - p_c) n_c - k_2^E n_2 \tag{37}$$

The rates of emission of the two volatile species are:

$$R_i^E = k_i^E n_i, \quad i = 1,2 \tag{38}$$

Using the dimensionless variables

$$\theta = k_c t \tag{39}$$

$$N_i = \frac{k_c n_i}{\eta_2 I_T^\circ}, \quad i = c,1,2 \tag{40}$$

The surface balances become:

$$\frac{dN_c}{d\theta} = f^\circ(\theta) + 1/\rho - N_c \tag{41}$$

$$\frac{dN_1}{d\theta} = 2p_c N_c - (k_1^E/k_c)N_1 \tag{42}$$

$$\frac{dN_2}{d\theta} = (1 - p_c)N_c - (k_2^E/k_c)N_2 \tag{43}$$

For the dc beam experiment, the output amplitude $\bar{\mathcal{Q}}_i$ is defined by:

$$\bar{\mathcal{Q}}_i = R_i^E = \eta_2 I_T^\circ \left(\frac{k_i^E}{k_c}\right) N_i, \quad i = 1,2 \tag{44}$$

and $f^\circ(\theta) = 1$, $dN_i/d\theta = 0$. The NiCl amplitude is

$$\bar{\mathcal{Q}}_1 = 2(1 + 1/\rho)\ \eta_2 I_T^\circ\ p_c \tag{45}$$

At high target temperatures, $\bar{\mathcal{A}}_1$ was observed to saturate, and $\bar{\mathcal{A}}_2$ vanished so that $p_c \to 1$ as $T \to \infty$. The amplitude attenuation factors are

$$\frac{\bar{\mathcal{A}}_1}{\left[\bar{\mathcal{A}}_1\right]_{T=\infty}} = p_c \tag{46}$$

and

$$\frac{\bar{\mathcal{A}}_2}{\left[\bar{\mathcal{A}}_1\right]_{T=\infty}} = \frac{1}{2}(1 - p_c) \tag{47}$$

Thus, only one item of information is obtainable from the dc beam experiments: the variation of p_c with target temperature.

In the modulated beam experiment, the output signal amplitudes are:

$$\mathcal{A}_i = \mathcal{F}\{R_i^E\} = \eta_2 I_T^\circ \left(\frac{k_i^E}{k_c}\right) \mathcal{F}\{N_i\}\ , \quad i = 1,2 \tag{48}$$

Since Eq. (41) is identical to the differential equation describing a simple first order desorption process, the solutions $N_{con}(\theta)$ and $N_{coff}(\theta)$ can be obtained from the considerations of Sec. I(b). Equation (42) can be integrated during the "on" and "off" periods using the appropriate expressions for $N_c(\theta)$ during each portion of the cycle. The constants of integration are determined by the usual matching technique. The Fourier coefficients of $N_1(\theta)$ are obtained from Eqs. (19) and (20), and $\mathcal{A}_1$ becomes:

$$\mathcal{A}_1 = \frac{4}{\pi}\ \eta_2 I_T^\circ\ p_c\ \frac{\theta_c}{(\pi^2 + \theta_c{}^2)^{1/2}}\ \frac{\theta_1}{(\pi^2 + \theta_1{}^2)^{1/2}} \tag{49}$$

where $\theta_1 = k_1^E t_c$ and $\theta_c = k_c t_c$.

At high target temperatures, $p_c \to 1$ and θ_c and $\theta_1 \to \infty$. The amplitude attenuation is:

$$\frac{\mathcal{Q}_1}{\left[\mathcal{Q}_1\right]_{T\to\infty}} = p_c \frac{\theta_c}{(\pi^2 + \theta_c^2)^{1/2}} \frac{\theta_1}{(\pi^2 + \theta_1^2)^{1/2}} \tag{50}$$

The phase shift with respect to the high temperature NiCl signal is

$$\tan \phi_1 = \left(-\frac{\pi}{\theta_c}\right)\left[\left(\frac{k_c + k_1^E}{k_1^E}\right) \frac{\theta_1^2}{\theta_1^2 - k_1^E \pi^2/k_c}\right] \tag{51}$$

For $NiCl_2$, the analogous results are:

$$\frac{\mathcal{Q}_2}{\left[\mathcal{Q}_1\right]_{T=\infty}} = \frac{1}{2}(1 - p_c) \frac{\theta_c}{(\pi^2 + \theta_c^2)^{1/2}} \frac{\theta_2}{(\pi^2 + \theta_2^2)^{1/2}} \tag{52}$$

$$\tan\phi_2 = \left(-\frac{\pi}{\theta_c}\right)\left[\left(\frac{k_c + k_2^E}{k_2^E}\right) \frac{\theta_2^2}{\theta_2^2 - k_2^E \pi^2/k_c}\right] \tag{53}$$

where $\theta_2 = k_2^E t_c$.

The amplitude attenuation ratios for the two volatile products are reduced by the product of two demodulation factors, which are absent from the dc equivalents, Eqs. (46) and (47). The phase shift formulae reflect the series resistances in each branch of the complex decomposition. If the desorption rate constants k_1^E or k_2^E are much larger than k_c, the phase lag is controlled by the rate at which the complex decomposes, and $\tan\phi_i = -(\pi/\theta_c)$, $i = 1,2$. On the other hand,

if desorption is slow compared to complex decomposition, $\tan\phi_i = -(\pi/\theta_i)$, $i = 1,2$.

The significant advantage of a modulated beam experiment over a dc experiment is in the fact that the left hand sides of Eqs. (50) - (53) represent four independent and experimentally obtainable pieces of information. The data permit determination of p_c, k_c, k_1^E, and k_2^E at each temperature. The dc experiment, however, yields only p_c.

One disadvantage of the modulated beam technique can be inferred from Eq. (52). The two demodulation factors for $NiCl_2$ act in opposite directions from the competition factor $(1 - p_c)/2$. At high temperatures, the demodulation factors approach unity, but so does p_c. At low temperatures, where nearly all of the incident chlorine returns to the gas as $NiCl_2$, the demodulation factors are small. In either extreme, the modulated output amplitude goes to zero. $NiCl_2$ can be expected to be found only at intermediate temperatures, and probably at amplitudes considerably smaller than NiCl. At a modulation frequency of 100 cps, Smith and Fite never observed $NiCl_2$. The loss of amplitude and phase information on $NiCl_2$ renders interpretation of the NiCl amplitude and phase shift data impossible, since Eqs. (50) and (51) contain three unknowns. The inability to detect modulated $NiCl_2$ at 100 cps points up the necessity of varying the modulation frequency in hunting for potential reaction products. Had lower modulation frequencies been tried, the product $NiCl_2$ might have been observed. However, the response of the lock-in amplifier deteriorates at low frequencies, and a digital signal-to-noise averager may be required.

III. Bulk Solution and Diffusion

In the preceding sections, the only removal mechanisms in the surface mass balances were evaporation or conversion to another adsorbed species. However, gases such as H_2, O_2, N_2, and CO show appreciable solubility in many metals, and at the elevated temperatures characteristic of many modulated beam experiments, diffusion of the dissolved gas in the target material may be rapid. Consequently, bulk solution and diffusion must be considered as a potential loss mechanism in the surface mass balance. Moore and Unterwald[3] have shown that solution and diffusion of hydrogen in tungsten and molybdenum dominated their flash filament experiments at temperatures above 1000°C.

Here we consider the case in which bulk solution-diffusion and rapid first order desorption are competitive processes. This restriction is valid for beams which adsorb without dissociation and do not react chemically with the substrate. This situation is also characteristic of the interaction of diatomic gases with metals at temperatures high enough such that bimolecular recombination is negligible compared to direct atom evaporation. At these temperatures, the mean life of an adsorbed atom is much smaller than the modulation time, so that the dn/dt term in the surface balance can be neglected. This simplification is analagous to the stationary intermediate assumption in homogeneous chemical kinetics.

Generally, modulated molecular beam experiments involve bombarding one side of a thin ribbon of target material with the beam. The back side of the target is subject only to bombardment by the

background gas. The higher impingement rate on the front face creates a concentration gradient of the dissolved species through the target. Such a net drain on the surface population results in a "competition factor" reducing the amplitude of the output signal from the lock-in amplifier (this component of the amplitude attenuation would be present in dc beam experiments as well). However, even if the competition factor were unity (by making the rear face of the target impervious to the dissolved gas), a reduction in the amplitude of the lock-in amplifier signal could result by demodulation due to the inability of the relatively slow bulk diffusional process to keep up with the periodic alteration of the supply of adsorbed atoms to the front surface. Since most molecular beam targets are of the thin ribbon variety, only the former case will be considered.

Let $c(x,t)$ denote the bulk concentration of dissolved gas (assumed to be the same form as the adsorbed species) at position x within the target and at a time t during one modulation cycle. Transport in the target is governed by the diffusion equation:

$$\frac{\partial c}{\partial t} = D_v \frac{\partial^2 c}{\partial x^2} \tag{54}$$

where D_v is the bulk diffusivity of the dissolved species in the target material and x is measured from the front face. We are interested in the process only after the initial transients due to starting up the beam or heating the target to temperature have died out. Consequently, the initial condition on Eq. (54) is replaced by the cyclic steady state condition:

$$c(x,t) = c(c,t + 2t_c) \tag{55}$$

In order to join the surface kinetic problem to the bulk diffusion problem, we assume that the concentration of the dissolved species just beneath the surface is proportional to the instantaneous surface concentration. For the front face of the target, this yields:

$$c(o,t) = H\, n(t) \tag{56}$$

where H is the solubility measured from the adsorbed state. In principle, H can be determined by combining the adsorption isotherm with the usual solubility based upon gas pressure.

The surface mass balance for the front face of the target constitutes one boundary condition on Eq. (54). Neglecting the dn/dt term and using Eq. (56), this is

$$\eta\, I_T^o\, f^o(t) = \frac{k_1^E}{H}\, c(o,t) - D_v \left(\frac{\partial c}{\partial x}\right)_o \tag{57}$$

Since the diffusion and evaporation processes are first order, the term reflecting the steady background $(1/\rho)$ has been neglected; this contribution is eliminated by the lock-in amplifier.

On the back face $(x = \ell)$ the supply term due to the beam is absent and the second boundary condition is:

$$0 = \frac{k_1^E}{H}\, c(\ell,t) + D_v \left(\frac{\partial c}{\partial x}\right)_\ell \tag{58}$$

While the diffusional term constitutes a loss to the front face, it represents a gain to the back face.

In order to solve Eq. (54) subject to (55), (57), and (58), the following dimensionless terms are introduced:

$$\theta = D_v t/\ell^2 \tag{59}$$

$$\xi = x/\ell \tag{60}$$

$$C(\xi,\theta) = \frac{D_v}{\eta\ I_T^o \ell}\ c \tag{61}$$

$$h = \frac{k_1^E \ell}{D_v H} \tag{62}$$

The diffusion equation and its associated conditions become:

$$\frac{\partial C}{\partial \theta} = \frac{\partial^2 C}{\partial \xi^2}, \quad 0 \leq \xi \leq 1, \quad -\theta_c \leq \theta \leq \theta_c \tag{63}$$

$$C(\xi,\theta) = C(\xi,\ \theta + 2\theta_c) \tag{64}$$

$$f^o(\theta) = h\ C(0,\theta) - \left(\frac{\partial C}{\partial \xi}\right)_o \tag{65}$$

$$0 = h\ C(1,\theta) + \left(\frac{\partial C}{\partial \xi}\right)_1 \tag{66}$$

where $\theta_c = D_v t_c/\ell^2$ is the ratio of the chopping time to the characteristic diffusion time of the system.*

* In this situation, there are three characteristic times: the chopping time t_c, the diffusion time $t_D = \ell^2/D_v$, and the evaporation time, $t_E = 1/k_1^E$. The analysis of this section is restricted to situations in which t_D and t_c are of comparable magnitude but both are much larger than t_E. Had the dn/dt term in the surface mass balance been retained, the first term on the right of Eq. (65) would have been replaced by $h[C(0,\theta)+(t_E/t_D)(\partial C/\partial\theta)_0]$. However, the last term of this expression is assumed to be small, since $t_E/t_D \ll 1$.

The amplitude of the output signal from the lock-in amplifier is due to evaporation from the surface, and can be written as:

$$\mathcal{Q}_1 = k_1^E \mathcal{F}\{n(t)\} = \eta\, I_T^\circ \mathcal{F}\{h\, C(0,\theta)\} \tag{67}$$

The surface mass balances have been written for a non-dissociating adsorption. For dissociative adsorption of a diatomic gas, the term $\eta\, I_T^\circ$ in Eqs. (57), (61), and (67) must be multiplied by two. The computed phase shifts and amplitude attenuation, however, are unaltered.

The solution to Eqs. (63) - (66) is presented in Appendix A, where the coefficients A and B of the fundamental modes of the Fourier expansion of $hC(0,\theta)$ are shown to be:

$$A = \frac{2}{\pi} \sum_{n=1}^{\infty} hb_n \frac{(\alpha_n^2\theta_c)\pi}{\pi^2 + (\alpha_n^2\theta_c)^2} \tag{68}$$

$$B = -\frac{2}{\pi} \left\{ \frac{1+h}{2+h} - \sum_{n=1}^{\infty} hb_n \frac{\pi^2}{\pi^2 + (\alpha_n^2\theta_c)^2} \right\} \tag{69}$$

where the b_n are given by:

$$b_n = \frac{2\alpha_n^2}{\alpha_n^2+h^2+2h} \left\{ \frac{1}{h}\,\frac{1+h}{2+h} \left[\sin\alpha_n - \frac{h}{\alpha_n}(\cos\alpha_n - 1) \right] - \frac{1}{\alpha_n}\,\frac{1}{2+h} \left[(\cos\alpha_n + \alpha_n \sin\alpha_n - 1) + \frac{h}{\alpha_n}(\sin\alpha_n - \alpha_n\cos\alpha_n) \right] \right\} \tag{70}$$

and the eigenvalues α_n are the roots of the transcendental equation:

$$\left[\left(\frac{\alpha_n}{2}\right) \tan\left(\frac{\alpha_n}{2}\right) - \frac{h}{2}\right]\left[\left(\frac{\alpha_n}{2}\right) \cot\left(\frac{\alpha_n}{2}\right) + \frac{h}{2}\right] = 0 \qquad (71)$$

As long as the combined activation energy of the permeability $D_v H$ is less than that of the rate constant for evaporation k_1^E (which is typically 50 kcal/mole), bulk solution-diffusion effects become less important as the temperature is increased (i.e., h becomes large at high target temperatures). Experimentally, this situation can be observed as a levelling off of the emission rate from the surface at high target temperatures, which signals an end to the competition between the two removal mechanisms in favor of evaporation. Comparing the output signal to the signal in the absence of bulk solution-diffusion ($h \to \infty$, $A \to 0$, $B \to -2/\pi$), the amplitude attenuation and phase shift are:

$$\frac{\mathcal{Q}_1}{\left[\mathcal{Q}_1\right]_{h\to\infty}} = \frac{\pi}{2}\left(A^2 + B^2\right)^{1/2} \qquad (72)$$

$$\phi_1 = \tan^{-1}(A/B) \qquad (73)$$

The results of the computations are plotted in Figs. 6 and 7 for a range of the parameters h and θ_c.

The response of the system is predominantly controlled by the parameter h. If either the diffusion coefficient or the solubility

is zero, $h \to \infty$, and bulk solution-diffusion does not affect the signal, irrespective of the value of the parameter θ_c.

As $h \to 0$ and $\theta_c \to \infty$ (infinite diffusivity, finite solubility), Eqs. (72) and (73) reduce to:

$$\frac{\left[\mathcal{A}_1\right]_{\substack{h\to 0\\ \theta_c\to\infty}}}{\left[\mathcal{A}_1\right]_{h\to\infty}} = \frac{1}{2}\,\frac{2h\theta_c}{[\pi^2 + (2h\theta_c)^2]^{1/2}} \tag{74}$$

$$\phi_1 = \tan^{-1}\left(-\frac{\pi}{2h\theta_c}\right) \tag{75}$$

where

$$h\theta_c = \frac{k_1^E t_c}{H\ell} \tag{76}$$

Except for the factor of 1/2 in Eq. (74), these amplitude attenuation and phase shift expressions are identical to Eqs. (33) and (34) for slow first order desorption, with k_1^E in the latter replaced by $2k_1^E/H\ell$. The product $H\ell$ represents the equilibrium capacity of the target for dissolved gas; it is the number of atoms in a square centimeter of target area when the surface concentration is unity. The foil acts as a holding tank for a portion of the atoms in the beam.

If $h\theta_c \to \infty$ while $h \to 0$, the target is characterized by infinite diffusivity but zero capacity. In this instance, the amplitude

attenuation reduces to 1/2 and the phase shift to zero. Physically this means that the incident beam is equally divided between the front and back faces of a transparent, zero capacity target. Evaporation from each face occurs at a rate one-half of the rate which would prevail if the target were impervious to the beam.

As the characteristic diffusion time becomes small compared to the chopping time ($\theta_c \rightarrow \infty$), the phase shift approaches zero, but an amplitude attenuation of magnitude $(h+1)/(h+2)$ remains. This limit is well represented by the $\theta_c = 1000$ curve on Fig. 6, its minimum value of 1/2. This term represents the time-average fraction of the atoms supplied to the surface which leave by evaporation. The remainder is lost by diffusion through the foil and emission from the rear face. This amplitude attenuation can be computed directly from the boundary conditions of Eqs. (57) and (58) by setting $f^{\circ}(t) = 1/2$ and the concentration gradient equal to $-(c(o)-c(\ell))/\ell$. Thus, $(h+1)/(h+2)$, is the "competition factor" in the amplitude attenuation, and is analogous to Eq. (30) for competitive first and second order reactions and p_c in the nickel-chlorine reaction. There is no demodulation factor when the chopping time is large compared to the diffusion time, and the phase shift is zero when $\theta_c \rightarrow \infty$.

When the chopping time and the diffusion time are of the same order of magnitude, the amplitude attenuation is reduced below $(h+1)/(h+2)$ due to demodulation of the signal. During the "off" portion of the cycle, the sluggish response of the bulk diffusion process continues to supply atoms to the surface layer even though the beam is off. The evaporation of these diffusion-supplied atoms during the "off" cycle reduces the ac amplitude of the emission rate waveform to which the lock-in amplifier responds, and hence reduces the magnitude of the output signal. The phase shift is no

longer zero.

As $\theta_c \rightarrow 0$, the signal is completely demodulated.

IV. Surface Diffusion

Localization of molecular beam impingement on a restricted area of the target implies that the amplitude and shape of the signal due to the reevaporated species can be affected by migration along the surface. If surface diffusion were very rapid compared to other loss mechanisms, the impinging beam would be instantaneously distributed over the entire heated area of the target instead of remaining in the region where the beam struck. Winterbottom and Hirth[7] have evaluated the effect of surface diffusion on the emission rate characteristics of hot molecular beam sources. Surface diffusion problems beset high temperature molecular beam experiments at both ends.

In this analysis, we assume that first order evaporation is the only other process with which surface diffusion is in competition. Consequently, the contribution of background gas impingement on the target can be neglected.

The total heated area of the target is assumed uniformly accessible to the mobile adatoms. Following Winterbottom,[7] edges and corners of the target (if any) are not considered to pose barriers to migration along the surface. The cool target supports, however, are assumed to present an impervious barrier to surface diffusion. The total heated area of the target (back as well as front faces if the target is a ribbon) is represented by a disk of radius r_0 at a uniform temperature. The radius r_0 is chosen such that πr_0^2 is equal to the total heated area of the target. The surface diffusion coefficient D_s and the evaporation

rate constant k_1^E are assumed constant over the entire hot target area. The impinging molecular beam is considered to have its maximum intensity at r = 0, and to diminish with increasing radial distance according to a prescribed function $F(r/r_0)$. $F(0)$ is unity, and in most target-beam geometries, F decreases to zero at some $r < r_0$.

The surface mass balance can be written in dimensionless terms as:

$$\frac{\partial N}{\partial \theta} = \frac{1}{\xi} \frac{\partial}{\partial \xi} \left(\xi \frac{\partial N}{\partial \xi}\right) + f^{\circ}(\theta)\, F(\xi) - \lambda N, \qquad 0 \leq \xi \leq 1 \tag{77}$$

The dimensionless terms in Eq. (77) are:

$$N = \left(\frac{D_s}{\eta \Gamma_T^{\circ} r_0^{\,2}}\right) n \tag{78}$$

$$\theta = D_s t / r_0^{\,2} \tag{79}$$

$$\xi = r/r_0 \tag{80}$$

$$\lambda = k_1^E r_0^{\,2} / D_s \tag{81}$$

The $\partial N/\partial \theta$ term has been retained in this analysis, since surface diffusion is generally significant at lower temperatures than bulk solution-diffusion; in the former case, the chopping, diffusion, and evaporation times may all be of the same order of magnitude.

The surface mass balance has been written for non-dissociative adsorption, but can be extended to diatomic gases by inserting a "2" in the denominator of Eq. (78).

The condition of cyclic steady state is:

$$N(\xi,\theta) = N(\xi,\ \theta + 2\theta_c) \tag{82}$$

and the boundary conditions are:

$$(\partial N/\partial \xi)_0 = 0 \tag{83}$$

$$(\partial N/\partial \xi)_1 = 0 \tag{84}$$

The output signal depends upon the instantaneous number density of the evaporating species in the ionizer of the mass spectrometer or other similar detector. The number density in the ionizer is the sum of contributions of emission from those portions of the target which offer a direct line of sight to the ionizer. Surface migration spreads the adatom population over a sizeable area of the target, some of which may be partially blocked off from direct view of the ionizer. Emission from such regions may not contribute as much to the total number density in the ionizer as the regions of the target at which the beam and detector are aimed. The instantaneous output signal from the detector is written as:

$$S(\theta) \sim \lambda \int_0^1 \xi\, G(\xi)\, N(\xi,\theta)\, d\xi \tag{85}$$

where $G(\xi)$ is a weighting function which accounts for the reduced contribution to the signal from off-center regions of the target (in particular, the back side of a ribbon target cannot contribute at all).

We assume that G is a function of radial position on the simplified disk-shaped target. For the interaction geometry shown in Fig. 1, this formulation is an oversimplification. The function $G(\xi)$ is considered specified.

The amplitude of the output signal from the lock-in amplifier is proportional to the fundamental mode of the Fourier transform of $S(\theta)$:

$$\mathcal{A} \sim \mathcal{F}\{S(\theta)\} \tag{86}$$

The coefficients of the fundamental mode are shown in Appendix B to be:

$$A = \lambda \sum_{n=0}^{\infty} \frac{k_n}{\alpha_n^2} \frac{(\alpha_n{}^2\theta_c)\pi}{\pi^2 + (\alpha_n{}^2\theta_c)^2} \tag{87}$$

$$B = -\lambda \sum_{n=0}^{\infty} \frac{k_n}{\alpha_n{}^2} \frac{(\alpha_n{}^2\theta_c)^2}{\pi^2 + (\alpha_n{}^2\theta_c)^2} \tag{88}$$

where:

$$k_n = \frac{1}{\pi} J_o^2(\beta_n) f_n g_n \tag{89}$$

f_n and g_n are the coefficients of the Fourier-Bessel expansions of the functions $F(\xi)$ and $G(\xi)$. The β_n are the roots of $J_1(\beta_n) = 0$ (where $\beta_0 = 0$). The α_n are given by:

$$\alpha_n^2 = \beta_n^2 + \lambda \tag{90}$$

If $\lambda \to \infty$, surface diffusion is insignificant compared to atom evaporation; if $(\lambda\theta_c) \to \infty$ as well, the surface residence time is small compared to the chopping time. Under these conditions, $A \to 0$ and $B \to -\sum_{n=1}^{\infty} k_n$. The amplitude attenuation is defined with respect to this limit:

$$\frac{\mathcal{Q}}{[\mathcal{Q}]_{\substack{\lambda \to \infty \\ (\lambda\theta_c) \to \infty}}} = \frac{(A^2 + B^2)^{1/2}}{\sum_{n=0}^{\infty} k_n} \tag{91}$$

The phase angle is

$$\phi = \tan^{-1}(A/B) \tag{92}$$

For the purpose of illustrative numerical calculation, we have taken the beam shape factor $F(\xi)$ and the response function $G(\xi)$ to be:

$$F(\xi) = G(\xi) = \begin{cases} 1, & 0 \leq \xi \leq R \\ 0, & R \leq \xi \leq 1 \end{cases} \tag{93}$$

This represents the common situation in which the beam is collimated to impinge as a circular spot of uniform intensity on part of the total target area. The detector has been assumed to view only this spot as well. R is the ratio of the beam spot radius to the equivalent radius of the heated target.

The amplitude attenuation and phase shift are functions of the parameters λ, θ_c and R. Figures 8-11 show numerical results of the amplitude attenuation and phase lag for representative values of these parameters.

For either very large or very small values of the parameter λ, the amplitude attenuation and phase shift can be written as:

$$\frac{\mathcal{A}}{[\mathcal{A}]_{\substack{\lambda\to\infty \\ (\lambda\theta_c)\to\infty}}} = J(R) \frac{(\lambda\theta_c)}{[\pi^2 + (\lambda\theta_c)^2]^{1/2}} \tag{94}$$

$$\phi = \tan^{-1}\left(\frac{\pi}{\lambda\theta_c}\right) \tag{95}$$

As $\lambda \to 0$, $J(R) \to R^2$, which is just the ratio of the beam spot area to the total heated target area. This limit represents the situation in which surface diffusion serves only to instantaneously distribute the impinging beam over the target. At $\lambda \to \infty$, $J(R)$ approaches unity, and surface diffusion is slow compared to both the desorption and modulation times; the deposited atoms never migrate beyond the boundaries of the beam spot.

The upper curves of Figs. 8 and 10 are equivalent to the limit as $\lambda\theta_c \to \infty$. Here, the modulation time is slow compared to surface diffusion and desorption; the phase shift is zero and the amplitude attenuation is:

$$\frac{\mathcal{A}_{(\lambda\theta_c)\to\infty}}{[\mathcal{A}]_{\substack{\lambda\to\infty \\ (\lambda\theta)\to\infty}}} = \frac{\sum_{n=0}^{\infty}\left[\frac{J_1(\beta_n R)}{\beta_n J_0(\beta_n)}\right]^2 \left(\frac{\lambda}{\lambda + \beta_n^2}\right)}{\sum_{n=0}^{\infty}\left[\frac{J_1(\beta_n R)}{\beta_n J_0(\beta_n)}\right]^2} \tag{96}$$

Equation (96) represents the "competition factor" for surface diffusion. While bulk solution-diffusion can reduce the surface population by no more than 50%, the reduction due to surface diffusion can be considerably greater since the limit of Eq. (96) as $\lambda \to 0$ is R^2.

The preceding results are based upon the assumption that the cooled periphery of the target is a perfect reflector for migrating adatoms. An equally acceptable boundary condition is to consider the outer edge of the target to act as a perfect sink for the diffusing species. In this case, Eq. (84) is replaced by $N(1,\theta) = 0$. The solutions for these two boundary conditions are very close for large values of λ (typically greater than 10); very few migrating adatoms reach the outer boundary before evaporating and the surface appears infinite in extent. However, there is a considerable difference in the curves at small λ. While the amplitude attenuation for $(\lambda\theta_c)\rightarrow\infty$ with a perfectly reflecting boundary approaches R^2 at small λ, it approaches zero in the same limit for a perfect sink at the outer boundary.

The implication throughout this discussion has been that surface diffusion represents a nuisance to molecular beam experiments because it reduces the magnitude of the measured signal. However, this need not be the case if one is interested in measuring surface diffusion coefficients at high temperatures. For a system in which only atom evaporation and surface migration can occur, measurement of the amplitude attenuation and phase lag in a well-defined beam-target-detector geometry can yield information on evaporation rate constants and surface diffusion coefficients.

In a similar manner, information on bulk solution and diffusion constants can be obtained by monitoring the emission from the back face of a ribbon target whose entire periphery has been rendered impervious to surface migration by suitable cooled barriers.

APPENDIX A

During a single "on" cycle ($-\theta_c < \theta < 0$), $f^\circ(\theta) = 1$ and Eqs. (63) to (66) can be written as:

$$\left.\frac{\partial C_{on}}{\partial \theta}\right| = \frac{\partial^2 C_{on}}{\partial \xi^2}, \quad -\theta_c \leq \theta \leq 0 \tag{A-1}$$

$$C_{on}(\xi, -\theta_c) = C_{off}(\xi, \theta_c) \tag{A-2}$$

$$-\left(\frac{\partial C_{on}}{\partial \xi}\right)_0 + h[C_{on}(0,\theta) - 1/h] = 0 \tag{A-3}$$

$$\left(\frac{\partial C_{on}}{\partial \xi}\right)_1 + h\, C_{on}\,(1,\theta) = 0 \tag{A-4}$$

where the cyclic condition of Eq. (64) has been replaced by a condition requiring that the concentration profiles at the beginning of the "on" cycle and at the end of the "off" cycle be identical. The solution to this set is:[8]

$$C_{on}(\xi,\theta) = u(\xi) + w(\xi,\theta) \tag{A-5}$$

$$u(\xi) = \frac{1}{h}\,\frac{1+h}{2+h} - \frac{1}{2+h}\,\xi \tag{A-6}$$

$$w(\xi,\theta) = \sum_{n=1}^{\infty} (a_{on,n} - b_n)\, X_n(\xi)\, e^{-\alpha_n^2(\theta+\theta_c)} \tag{A-7}$$

The eigenvalues α_n are given by Eq. (71) in the text, and the eigenfunctions are:

$$X_n(\xi) = \cos(\alpha_n \xi) + \frac{h}{\alpha_n} \sin(\alpha_n \xi) \tag{A-8}$$

The $a_{on,n}$ are the coefficients in the eigenfunction expansion of $C_{on}(\xi, -\theta_c)$:

$$C_{on}(\xi, -\theta_c) = \sum_{n=1}^{\infty} a_{on,n} \; X_n(\xi)$$

$$a_{on,n} = \frac{2\alpha_n^2}{\alpha_n^2 + h^2 + 2h} \int_0^1 C_{on\,n}(\xi, -\theta_c) \, X_n(\xi) \, d\xi \tag{A-9}$$

The b_n are the coefficients of the eigenfunction expansion of $u(\xi)$:

$$u(\xi) = \sum_{n=1}^{\infty} b_n X_n(\xi)$$

$$b_n = \frac{2\alpha_n^2}{\alpha_n^2 + h^2 + 2h} \int_0^1 u(\xi) \, X_n(\xi) \, d\xi \tag{A-10}$$

The complete expression for b_n is given as Eq.(70) in the text.

During the "off" cycle $(0 < \theta < \theta_c)$, $f^\circ(\theta) = 0$ and Eqs. (63) to (66) become:

$$\frac{\partial C_{off}}{\partial \theta} = \frac{\partial^2 C_{off}}{\partial \xi^2} \;, \qquad 0 \le \theta \le \theta_c \tag{A-11}$$

$$C_{off}(\xi,0) = C_{on}(\xi,0) \tag{A-12}$$

$$-\left(\frac{\partial C_{off}}{\partial \xi}\right)_0 + h\, C_{off}(0,\theta) = 0 \tag{A-13}$$

$$\left(\frac{\partial C_{off}}{\partial \xi}\right)_1 + h\, C_{off}(1,\theta) = 0 \tag{A-14}$$

The solution is:

$$C_{off}(\xi,\theta) = \sum_{n=1}^{\infty} a_{off,n}\, X_n(\xi)\, e^{-\alpha_n^2\theta} \tag{A-15}$$

where X_n and α_n are the same as before, and $a_{off,n}$ are the coefficients of the eigenfunction expansion $C_{off}(\xi,0)$:

$$C_{off}(\xi,0) = \sum_{n=1}^{\infty} a_{off,n}\, X_n(\xi)$$

$$a_{off,n} = \frac{2\alpha_n^2}{\alpha_n^2+h^2+2h} \int_0^1 C_{off}(\xi,0)\, X_n(\xi)\, d\xi \tag{A-16}$$

Utilizing the matching conditions, Eqs. (A-2) and (A-12) yields:

$$a_{on,n} - b_n = -\frac{b_n}{1 + e^{-\alpha_n^2\theta_c}} \tag{A-17}$$

$$a_{off,n} = \frac{b_n}{1 + e^{-\alpha_n^2\theta_c}} \tag{A-18}$$

Substituting Eq. (A-17) into (A-7) and (A-18) into (A-15) yields the solutions for $C_{on}(\xi,\theta)$ and $C_{off}(\xi,\theta)$. The desired forms of the solutions are the coefficients of the fundamental modes of the Fourier expansion of $hC(0,\theta)$ [Eqs. (19) and (20) with $N(\theta)$ replaced by $hC(0,\theta)$]. These are given by Eqs. (68) and (69) in the text.

APPENDIX B

During the "on" cycle, Eq. (77) is:

$$\frac{\partial N_{on}}{\partial \theta} = \frac{1}{\xi} \frac{\partial}{\partial \xi} \left(\xi \frac{\partial N_{on}}{\partial \xi} \right) + F(\xi) - \lambda N_{on}, \quad -\theta_c \leq \theta \leq 0 \tag{B-1}$$

and the boundary conditions are:

$$(\partial N_{on}/\partial \xi)_0 = 0 \tag{B-2}$$

$$(\partial N_{on}/\partial \xi)_1 = 0 \tag{B-3}$$

The solution to Eq. (B-1) which satisfies Eqs. (B-2) and (B-3) is:

$$N_{on} = \sum_{n=0}^{\infty} \left(b_n + c_n e^{-\alpha_n^2 \theta} \right) J_o(\beta_n \xi) \tag{B-4}$$

where the b_n are given by:

$$b_n = f_n/\alpha_n^2 \tag{B-5}$$

and α_n^2 is given by Eq. (90) in the text. The β_n are the zeros of the Bessel function of the first kind of order one. The coefficients f_n are:

$$f_n = \frac{2 \int_0^1 \xi \, F(\xi) \, J_o(\beta_n \xi) \, d\xi}{J_o^2(\beta_n)} \tag{B-6}$$

During the "off" portion of the cycle, Eq. (77) is:

$$\frac{\partial N_{off}}{\partial \theta} = \frac{1}{\xi}\frac{\partial}{\partial \xi}\left(\xi \frac{\partial N_{off}}{\partial \xi}\right) - \lambda N_{off}, \quad 0 \leq \theta \leq \theta_c \tag{B-7}$$

with boundary conditions analagous to Eqs. (B-2) and (B-3). The solution can be written as:

$$N_{off} = \sum_{n=0}^{\infty} a_n e^{-\alpha_n^2 \theta} J_o(\beta_n \xi) \tag{B-8}$$

The unknown coefficients c_n and a_n are obtained from the matching conditions:

$$N_{on}(\xi, -\theta_c) = N_{off}(\xi, \theta_c) \tag{B-9}$$

$$N_{on}(\xi, 0) = N_{off}(\xi, 0) \tag{B-10}$$

These yield:

$$a_n = \frac{f_n}{\alpha_n^2} \frac{e^{\alpha_n^2 \theta_c}}{1 + e^{\alpha_n^2 \theta_c}} \tag{B-11}$$

$$c_n = -\frac{f_n}{\alpha_n^2} \frac{1}{1 + e^{\alpha_n^2 \theta_c}} \tag{B-12}$$

Inserting the solutions for N_{on} and N_{off} into Eq. (85) of the text and determining the coefficients A and B by replacing $N(\theta)$ in Eqs. (19) and (20) by $S(\theta)$ yields Eqs. (87) and (88) of the text. The coefficients g_n are given by Eq. (B-6) with $F(\xi)$ replaced by $G(\xi)$.

ACKNOWLEDGMENTS

The author would like to thank P. Concus and L. Wilson for their help in the computations.

This work was performed under the auspices of the United States Atomic Energy Commission.

REFERENCES

1. J. N. Smith and W. L. Fite, in Advances in Rarefied Gas Dynamics, J. A. Laurmann, Editor, Vol. 1, Suppl. 2, (Academic Press, New York, 1963), p. 430.
2. R. A. Krakowski and D. R. Olander, USAEC Report, UCRL-17336-rev, University of California, Berkeley, to be published in J. Chem. Phys.
3. G. E. Moore and F. C. Unterwald, J. Chem. Phys. 40, 2626, 2639 (1964).
4. J. D. McKinley, J. Chem. Phys. 40, 120 (1964).
5. S. Yamamoto and R. E. Stickney, J. Chem. Phys. 47, 1091 (1967).
6. J. Perel, R. H. Vernon and H. L. Daley, J. Appl. Phys. 36, 2157 (1965).
7. W. L. Winterbottom, J. Chem. Phys. 47, 3546 (1967); W. L. Winterbottom and J. P. Hirth, J. Chem. Phys. 37, 784 (1962).
8. H. S. Carslaw and J. C. Jaeger, Conduction of Heat in Solids, 2nd Ed., (Oxford Press, New York, 1959), p. 114, 118.

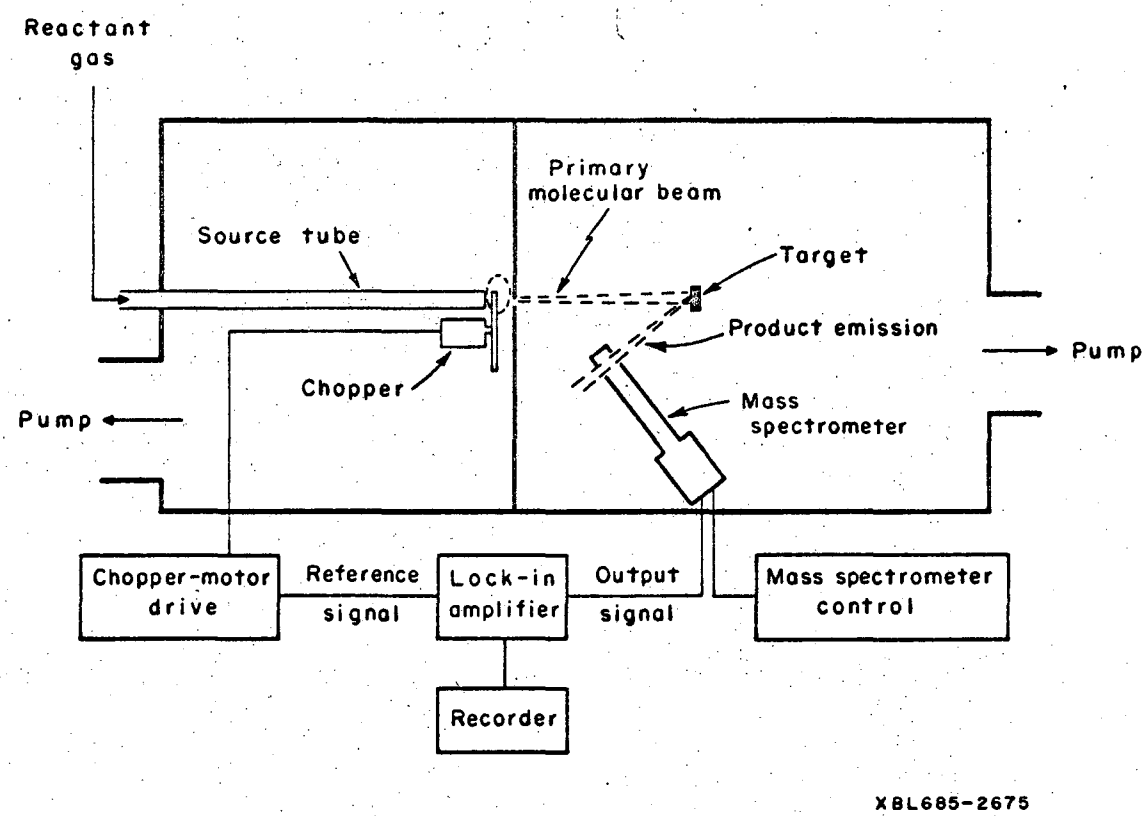

Fig. 1 Schematic diagram of molecular beam apparatus.

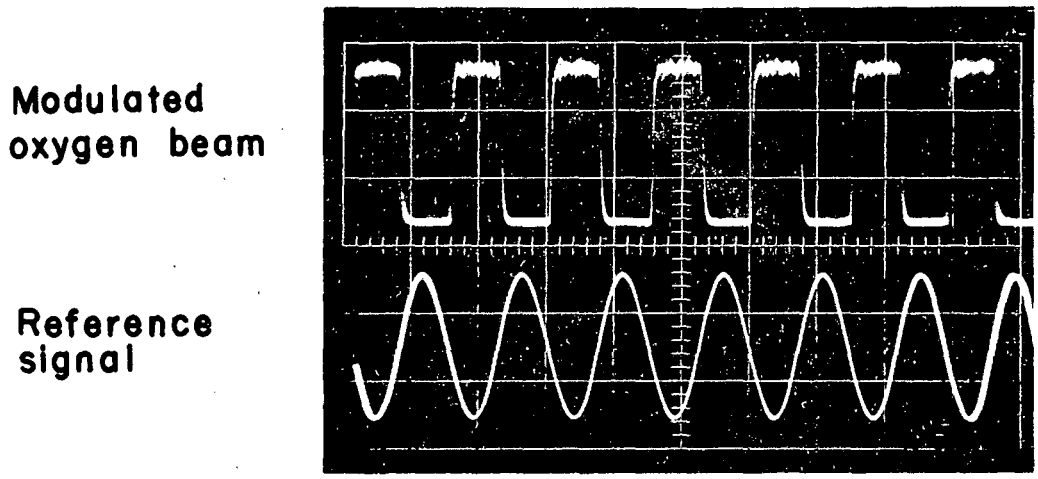

XBB 6710-6262-A

Fig. 2 Oscilloscope trace of primary molecular beam modulated at 145 cps.

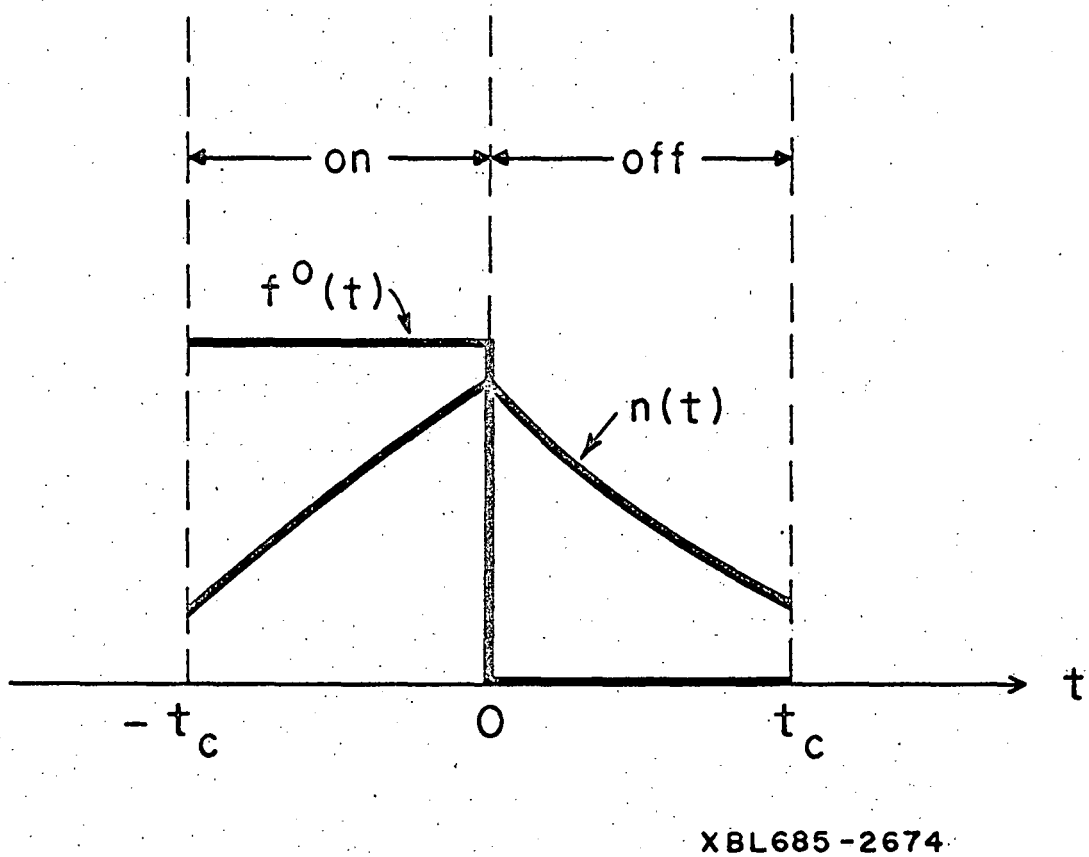

Fig. 3 Variation of surface concentration during a modulation cycle.

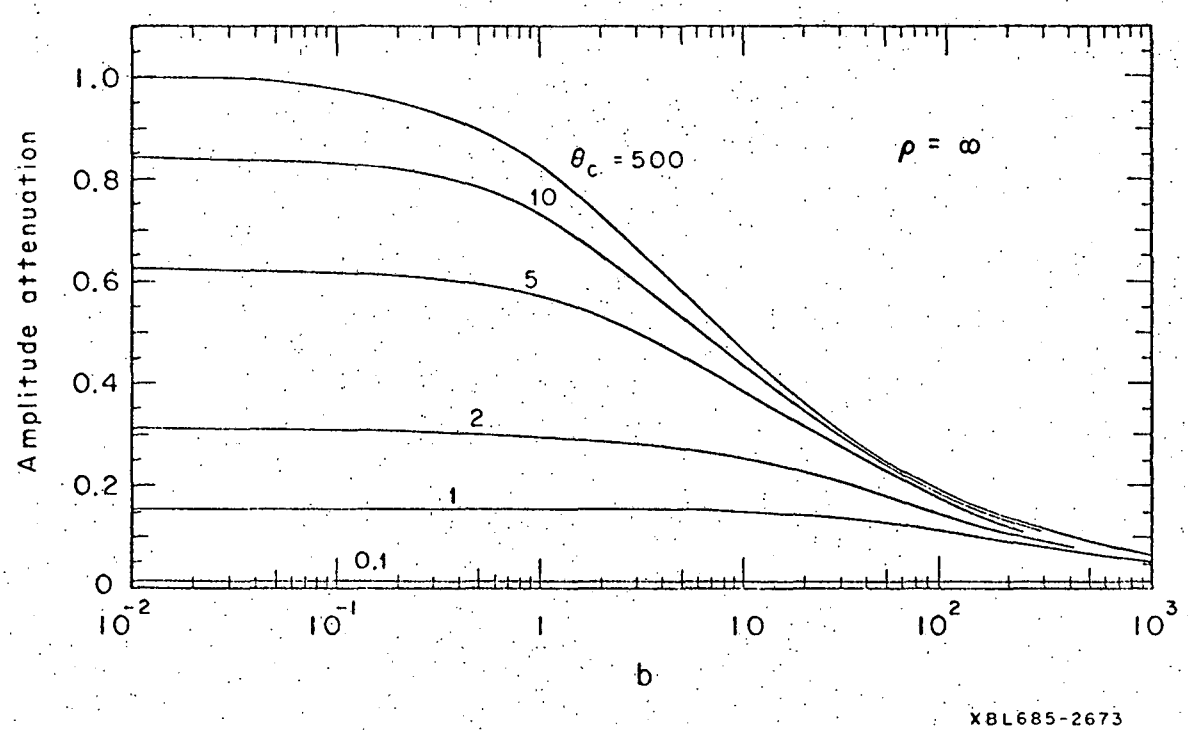

Fig. 4 Amplitude attenuation of lock-in detector signal for slow competitive first and second order reactions with no background contribution.

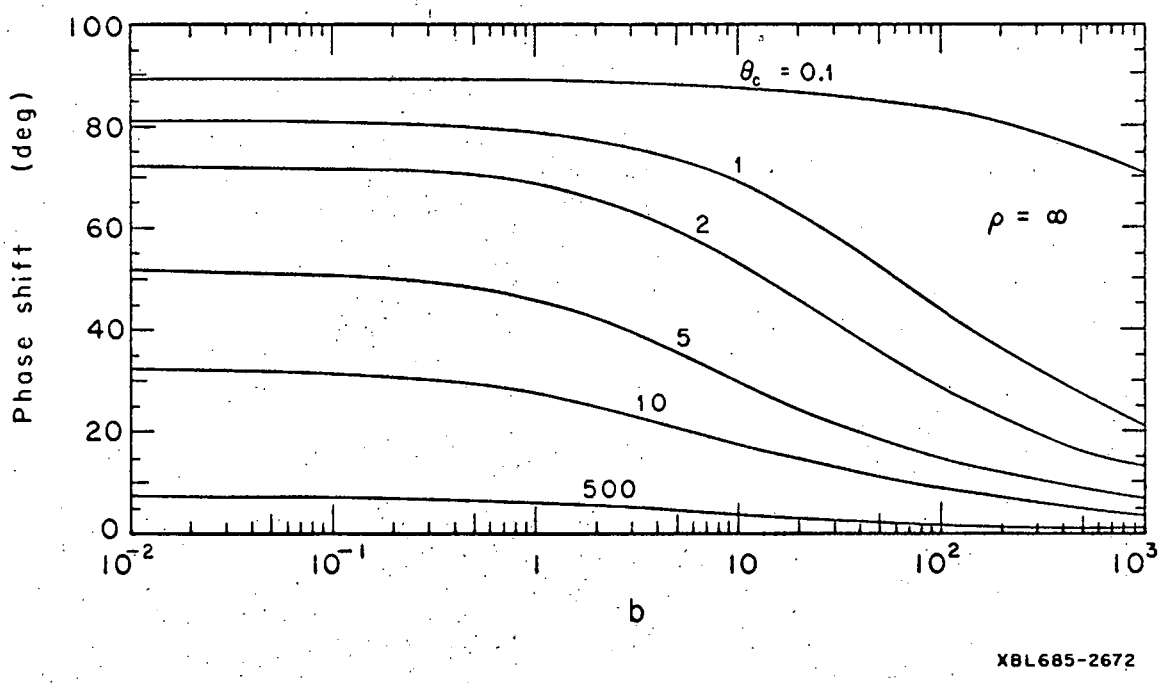

Fig. 5 Phase shift of lock-in detector signal for slow competitive first and second order reactions with no background contribution.

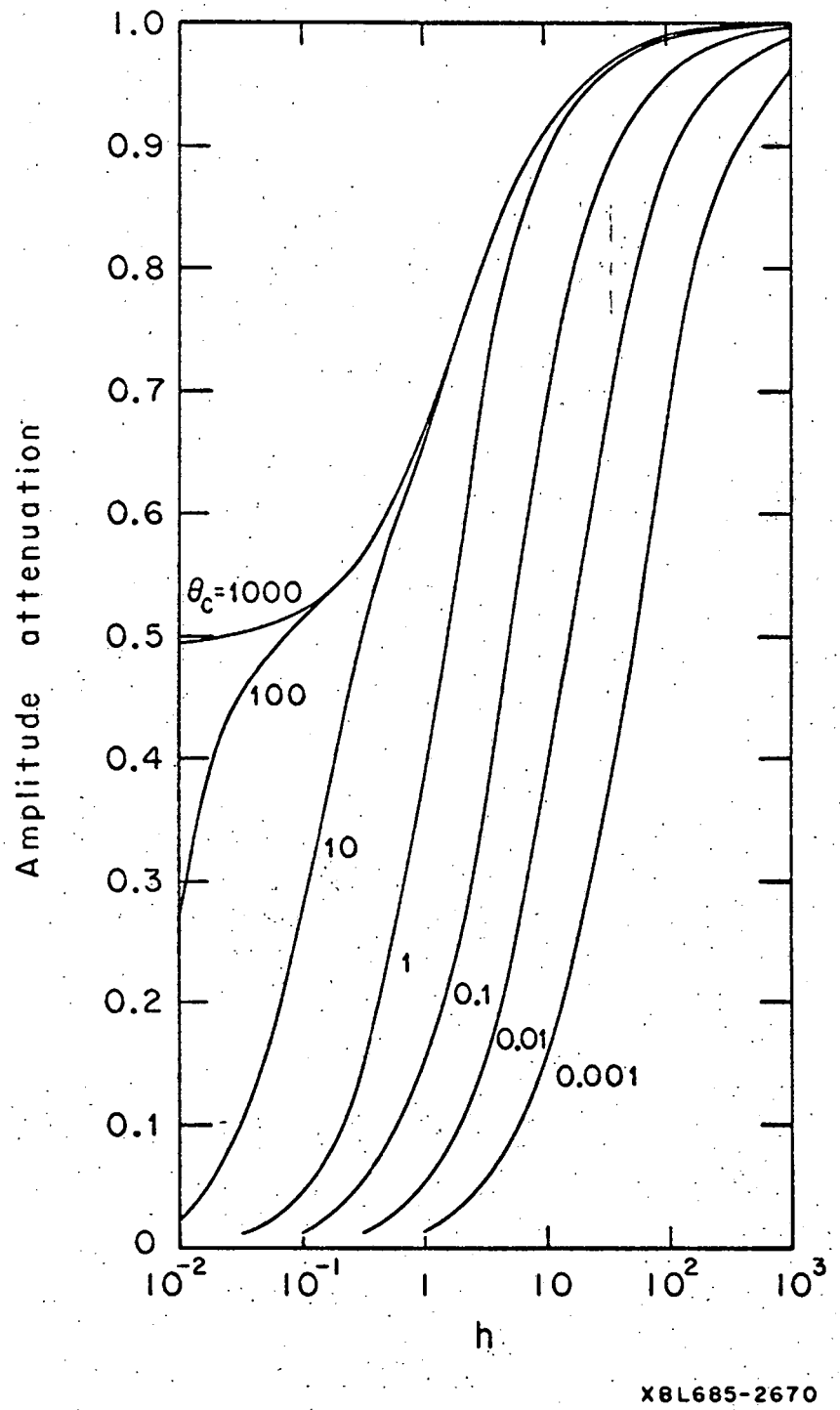

Fig. 6 Amplitude attenuation of lock-in detector signal for competitive rapid first order desorption and bulk solution-diffusion.

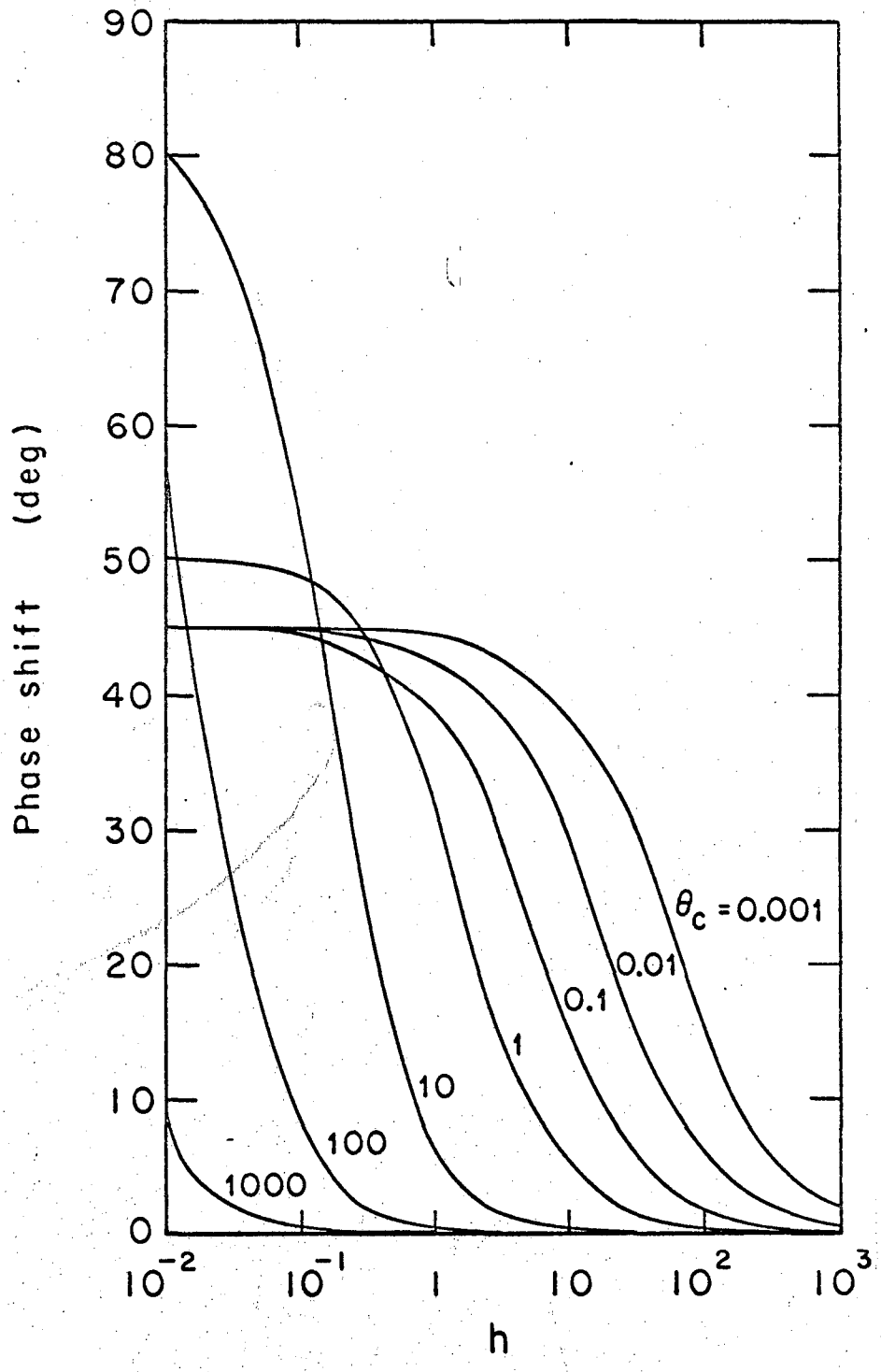

XBL685-2671

Fig. 7 Phase shift of lock-in detector signal for competitive rapid first order desorption and bulk solution-diffusion.

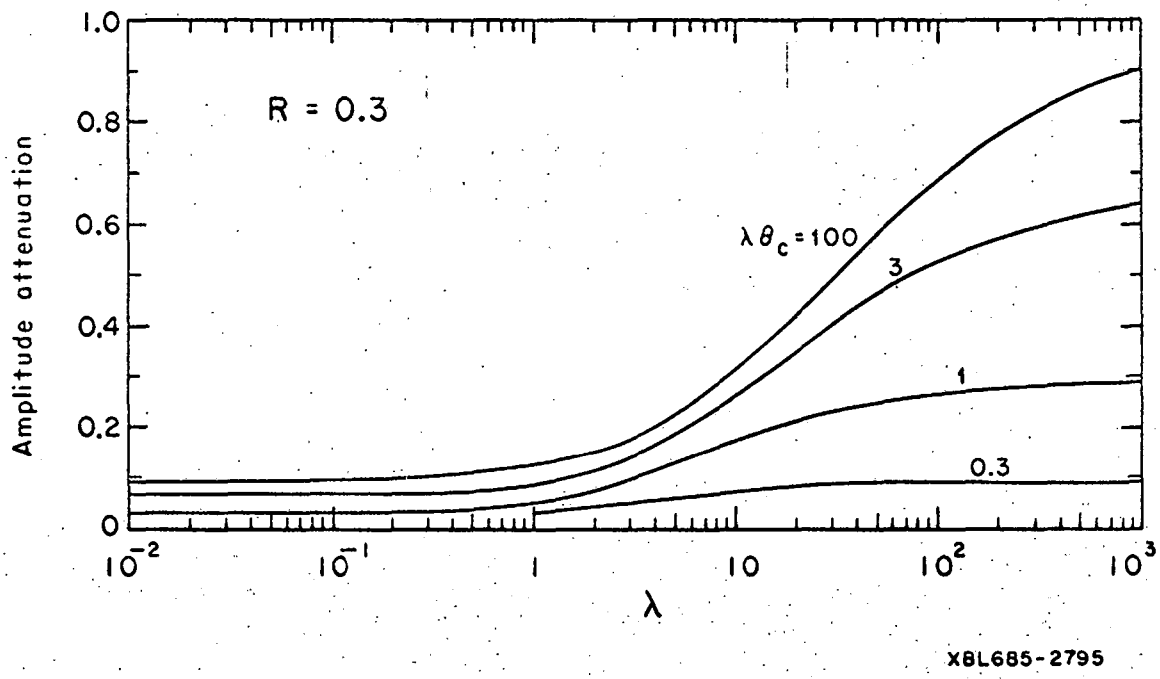

Fig. 8 Amplitude attenuation of lock-in detector signal for competitive slow first order desorption and surface diffusion. R = 0.3.

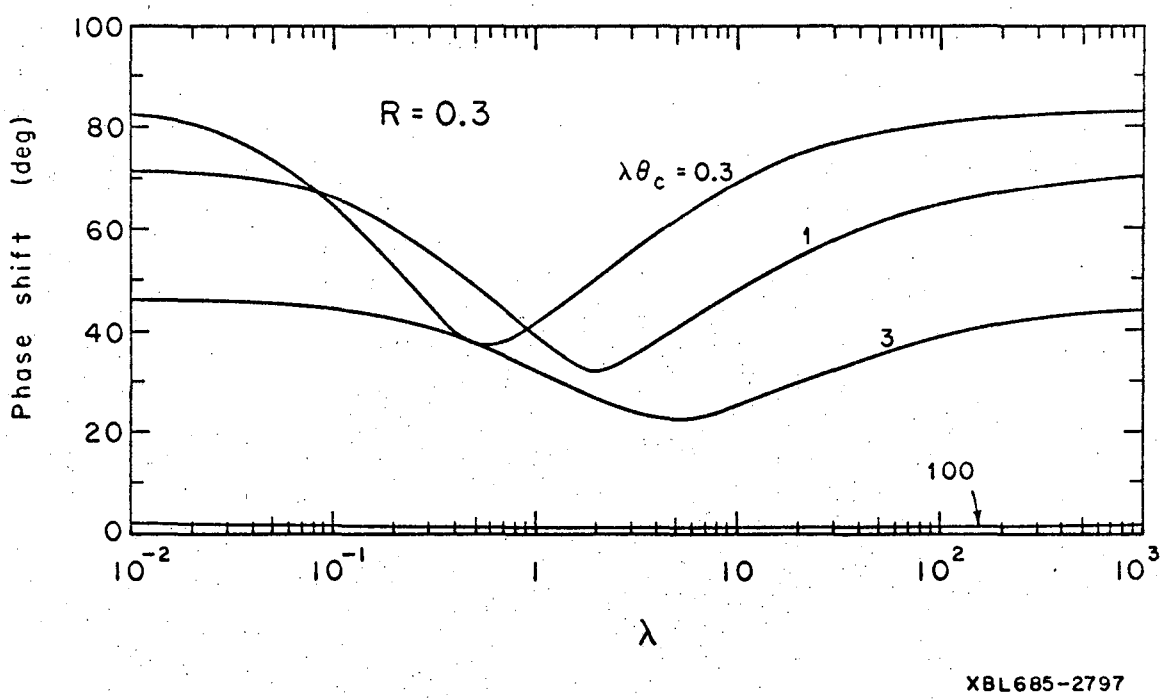

Fig. 9 Phase shift of lock-in detector signal competitive slow first order desorption and surface diffusion. R = 0.3.

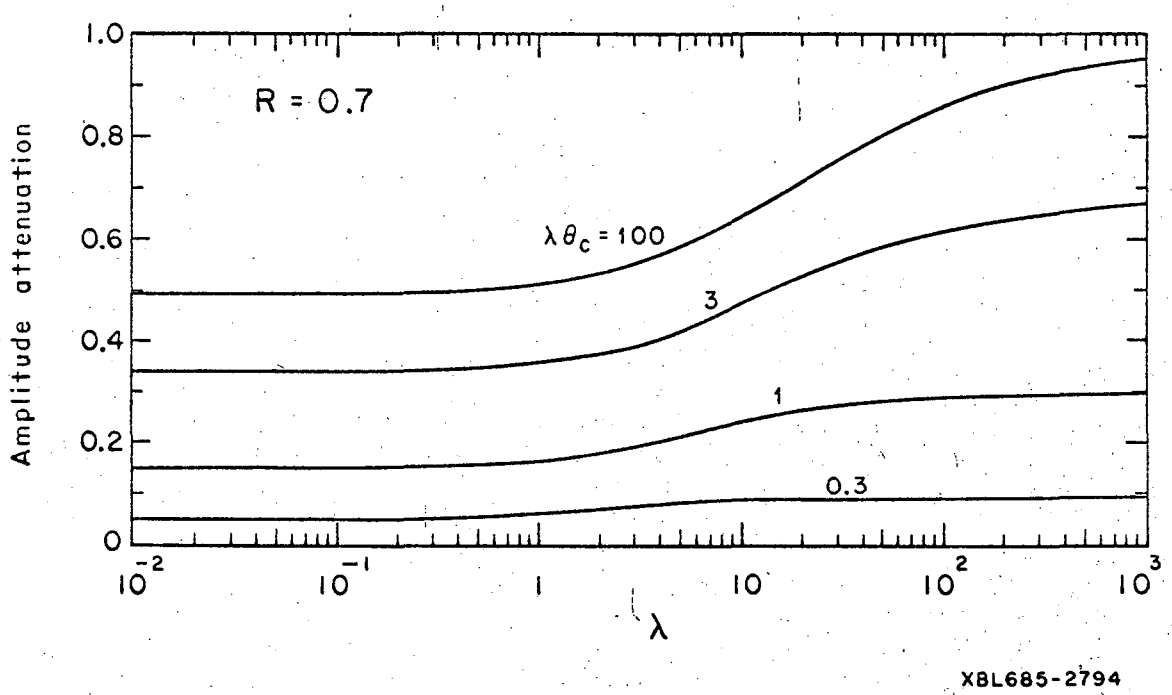

Fig. 10 Amplitude attenuation of lock-in detector signal for competitive slow first order desorption and surface diffusion. R = 0.7.

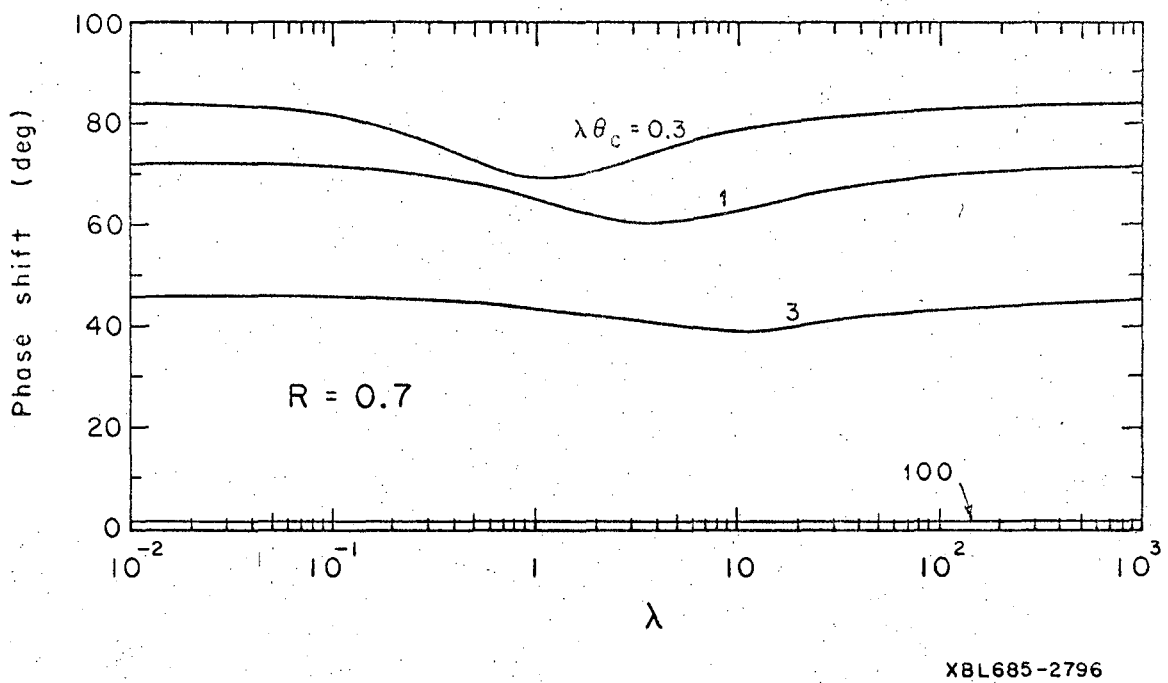

Fig. 11 Phase shift of lock-in detector for competitive slow first order desorption and surface diffusion. R = 0.7.

This report was prepared as an account of Government sponsored work. Neither the United States, nor the Commission, nor any person acting on behalf of the Commission:

A. Makes any warranty or representation, expressed or implied, with respect to the accuracy, completeness, or usefulness of the information contained in this report, or that the use of any information, apparatus, method, or process disclosed in this report may not infringe privately owned rights; or

B. Assumes any liabilities with respect to the use of, or for damages resulting from the use of any information, apparatus, method, or process disclosed in this report.

As used in the above, "person acting on behalf of the Commission" includes any employee or contractor of the Commission, or employee of such contractor, to the extent that such employee or contractor of the Commission, or employee of such contractor prepares, disseminates, or provides access to, any information pursuant to his employment or contract with the Commission, or his employment with such contractor.